A new exact numerical series for the determination of the Biot number: Application for the inverse estimation of the surface heat transfer coefficient in food processing.

Francisco J. Cuesta*, Manuel Lamúa & Rafael Alique
Department of Products
Institute of Food Science, Technology and Nutrition, ICTAN-C.S.I.C.
José Antonio Novais, 10
Ciudad Universitaria
28040 Madrid (Spain)

Abstract

As a corollary to a previous work, a new exact numerical series is deduced for the Biot number for the case of elementary geometries. This series is rapidly converging, allowing a very accurate approximation when truncated at its first term.

On the basis of this first approximation to the series, the equation is generalized and proposed to indirectly estimate the Biot number for regular geometries.

Keywords: Surface heat transfer coefficient, inverse methods

Nomenclature

A_n= Series expansion constants

$a = k/(\rho c)$ Thermal diffusivity ($\mathrm{m^2 s^{-1}}$)

$Bi = hR/k$ = Biot number

$Fo = at/R^2$ = Fourier number

h = Surface heat transfer coefficient ($\mathrm{Wm^{-2}K^{-1}}$)

J_0 = Zeroth-order Bessel function of first kind

J_1 = First-order Bessel function of first kind

K, K_δ = Geometry-dependent constants

k = Thermal conductivity ($\mathrm{Wm^{-1}K^{-1}}$)

$L = 2X_1$ = Major axis of the ellipsoid (m)

$R = X_3$ = Shortest body length (m)

T = Temperature (ºC)

T_{ex} = Temperature of the medium (ºC)

T_0 = Initial temperature (ºC)

X_1, X_2, X_3 = Semi axes of the ellipsoid (m)

$x = r/R$ = Dimensionless distance from the centre

$Y = (T - T_{ex})/(T_0 - T_{ex})$ = Dimensionless ratio of temperature difference

$\bar{Y} = (\bar{T} - T_{ex})/(T_0 - T_{ex})$ = Dimensionless ratio of mass average temperature difference

Greek letters

α^2 = Dimensionless slope of the heat source

β = Dimensionless number of the heat source

δ_n = Solutions to the transcendental equation of boundary condition

$\Gamma = SR/V$ = Geometric constant

$\omega_1 = X_3/X_1$; $\omega_2 = X_3/X_2$; $\omega = R/L$ = Shape parameters

$\psi = \psi(\delta_n x)$ = the spatial component of the solution in Fourier series expansion

Subscripts

* Corresponding author. Tel.: (0034) 915 445 607 | Fax. 0034 915 493 627; e-mail: fcb@ictan. csic. es

1 = First term in infinite series
c = Value on the centre
j = Index of geometric component
M = Value when $Bi \to \infty$
n = Index in infinite series

1. Introduction

The surface heat transfer coefficient h is a key parameter in the calculation of heating/chilling time, and hence in the design of facilities for thermal treatments of foods (hydro-cooling, air-cooling, cooking, etc.). In heat transfer it acts in boundary conditions (of the third kind) governed by Newton's law of cooling [1], according to whom the amount of heat $d\dot{Q}$ per unit of time that passes through a surface element dS which is at the temperature T_S, to an external medium which is at the temperature T_{es} is governed by the equation:

$$d\dot{Q} = h(T_S - T_{ex})dS \quad (1)$$

This parameter is external to the solid body being cooled/heated, but it determines its (internal) cooling/heating rate. It is linked to the boundary layer between the solid itself and the external fluid that extracts/inputs heat [2], [3]. Its value depends on the geometry of the body, the friction coefficient and the physical properties and velocity of the fluid. To determine that value it is necessary to ascertain the energy that is exchanged with the body, as done for example by Kwon et al. [4], who use a naphthalene sublimation technique to measure the heat yielded by the body.

Normally the surface transfer coefficient is measured indirectly, as reported in the reviews [5] and [6]. In elementary geometries, if the time-temperature history is measured experimentally at a certain point, the Biot number can be derived indirectly. This method has been used by numerous authors in Food Engineering as seen, for example, in [5], [7]-[11]. The method is based on the linear approximation reached on a semi-logarithmic scale by the temperature history after an initial time. Conduction should then be considered in a simply-shaped, homogeneous and isotropic solid suddenly immersed in a moving fluid at temperature T_{ex}. If the body is initially at a uniform temperature T_0 and there is no internal heat generation, the separate-variables solution to the equation for heat transfer by conduction in elementary geometries is given by the sum of a series of infinite terms [12]. In practice, this series converges rapidly and, after a certain time has elapsed ($Fo > 0.2$ [5]), only the first series term is significant, and the infinite series may be approximated to its first term. On a semi-logarithmic scale this can be plotted by means of a straight line:

$$\ln Y = \ln A - \delta^2 Fo \quad (2)$$

The constant δ depends on the geometric shape and the exchange of heat with the external medium (Biot number, Bi), but not on the internal position of the body. Actually, δ is the first solution of the boundary layer transcendental equation:

$$-\delta\psi'_\delta = Bi\psi_\delta \quad (3)$$

Which is the dimensionless expression of equation (1). Bi is the ratio between internal and external resistances and represents the dimensionless surface heat transfer coefficient h. Constant A is the "lag factor", which depends both on the Biot number and the internal position of the point in the body. In the case of elementary geometries its explicit expression is:

$$A = A_1\psi(\delta x) \quad (4)$$

Where A_1 is the first of the series expansion coefficients of the complete solution and function $\psi(\delta_n x)$ is the spatial component of the solution ($\cos(\delta_n x)$ for an infinite slab, $J_0(\delta_n x)$ for an infinite cylinder and $\sin(\delta_n x)/(\delta_n x)$ for a sphere) [12].

So, if the time-temperature history is measured experimentally at a certain point, the slope δ^2 may be obtained by empirical linear regression and this value can be used to determine Bi by solving in equation (3). This is called the "rate method" [8]. Or if the lag factor A is determined simultaneously at the centre

and at another point inside the body with a dimensionless coordinate $0 < x < 1$, the value of the Biot number can likewise be determined- This is called the ratio method [8]. In fact, if the lag factor is measured at the geometric centre ($x = 0$), since at this point $\psi = 1$, the lag factor is $A = A_1\psi(0) = A_1$. For $0 < x < 1$, its value is (Eq. 4) $A = A_1\psi(\delta x)$. Hence, if both values of A are divided, the value of the function $\psi(\delta x)$ can be found. Then, by applying equation (3), the Biot number —that is the value of the surface heat transfer coefficient— can also be determined.

For more complex geometries (irregular and three-dimensional in general) or for heterogeneous or anisotropic solids, a numerical calculation is required for inverse evaluation of the surface heat transfer coefficient. In this connection, as seen, for example in [13] (time-dependent heat transfer coefficient), [14]- [16], and [17] (who additionally use an iterative process to evaluate the spatial distribution of the surface heat transfer coefficient).

This paper presents a new general numerical series for the Biot number, which is mathematically exact in the case of the three elementary geometries, from which it is possible to deduce a first, highly precise approximation by truncating the series at its first partial summation. This approximation is generalized to other geometries on the basis of the regular geometries (parallelepiped and finite cylinder).

2. Numerical series for elementary geometries

As shown in the Appendix A, the function $\psi(\delta)$ and the ratio $-\psi'(\delta)/\psi(\delta)$ can be written for the three elementary geometries as exact numerical series in the form:

$$\frac{1}{\psi(\delta)} = 1 + \sum_{n=1}^{\infty} A_{n,M} \frac{\delta^2}{\delta_{n,M}^2 - \delta^2} \tag{5}$$

Where:

$$A_{n,M} = \frac{-2}{\delta_{n,M}\psi'(\delta_{n,M})}$$

$$\frac{-\psi'(\delta)}{\psi(\delta)} = \delta\left[\frac{1}{(\Gamma+1)} + \sum_{n=1}^{\infty} \frac{2}{\delta_{n,M}^2} \times \frac{\delta^2}{\delta_{n,M}^2 - \delta^2}\right] \tag{6}$$

Be it remembered that $\psi(\delta) = \cos\delta$ and $-\psi'(\delta)/\psi(\delta) = \tan\delta$ for the flat plate; $\psi(\delta) = J_0(\delta)$ and $-\psi'(\delta)/\psi(\delta) = J_1(\delta)/J_0(\delta)$ for the infinite cylinder; and $\psi(\delta) = \sin\delta/\delta$ and $-\psi'(\delta)/\psi(\delta) = 1/\delta - \cot\delta$ for the sphere. By substituting equation (6) in equation (3) the Biot number can be solved, leaving the exact numerical series:

$$Bi = \frac{hR}{k} = \delta^2\left[\frac{1}{(\Gamma+1)} + \sum_{n=1}^{\infty} \frac{2}{\delta_{n,M}^2} \times \frac{\delta^2}{\delta_{n,M}^2 - \delta^2}\right] \tag{7}$$

$(\Gamma + 1)$ is the geometric constant (1 for infinite slab, 2 for an infinite cylinder and 3 for a sphere) and $\delta_{n,M}$ are the values of δ_n when $Bi \to \infty$: $\delta_{n,M} = (2n-1)\pi/2$ for Infinite slab; $\delta_{n,M} = n\pi$ for the Sphere. In the case of an infinite cylinder, the values have been tabulated. Table I shows the first 20 roots $\delta_{n,M}$ for the infinite cylinder, and also the corresponding values of J_1 [18].

Table 1.

It follows that series (7) is mathematically exact for elementary geometries, the same as series (6) from which it is derived. As it can be seen, its value depends only on the slope δ^2 and global geometric factors, but is not dependent on internal position in the body, nor (explicitly) of the function $\psi(\delta)$ corresponding to each particular geometry. Its dependence on the latter is mediated by its geometric constant $(\Gamma + 1)$ and by the maximum values of δ ($\delta_{n,M}$).

Thus, these series serve to derive the Biot number for elementary geometries from the slope of the $\ln(Y) - Fo$ line. Its validity is shown in Fig. 1, where the Biot number, calculated from series (7), is plotted on the y-axis versus the real Biot number (on the x-axis). In all three geometries series (7) should lead to a single diagonal, which is depicted with solid line in Fig. 1.
Fig. 1.
Fig. 2.
Fig. 3.

3. First approximations to numerical series (7)

3.1. Estimation of the Biot number in elementary geometries

Series (6) is very rapidly convergent, and hence so is series (7) derived from it. Fig. 2 shows the deviation (%) of the partial series as a function of the number of terms taken for the sum. The reference Biot number is $Bi = 4$ in all three geometries, since, as will be seen in Fig. 3, $Bi = 4$ is approximately the value for which is the error is maximum. As can be seen in Fig. 2, the convergence is very rapid, and in any case this is always an approximation by default (value smaller than the exact value), since in any case (7) is a monotonically increasing series. The maximum error introduced in the inverse calculation of the Biot number from the value of the slope δ^2, taking as an approximation the partial sum reduced to the first term, is -1.77% for the sphere, -1% for the cylinder and -0.33% for the infinite plate. In any case the error will be less than -1.8% in the three elementary geometries, which, given that often the thermophysical constants are known with a greater degree of inaccuracy is a reasonable approximation in Food Engineering [19]. This is clearly illustrated in Fig. 3, which shows the error (%) produced by taking the first approximation for elementary geometries (Equation 8, below) as a function of the logarithm of the Biot number. As seen, the maximum error is indeed around $Bi = 4$ and diminishes rapidly to either side of this value. In this way the complete series can be approximated by means of the first partial series and thus approximate the Biot number by means of its first two terms:

$$Bi = \frac{hR}{k} \approx \delta^2 \left[\frac{1}{(\Gamma + 1)} + \frac{2}{\delta_M^2} \times \frac{\delta^2}{\delta_M^2 - \delta^2} \right] \tag{8}$$

In this equation, Bi depends on the slope δ^2 and on the two constants that depend only on the geometry: $(\Gamma + 1)$ and δ_M^2.

Adding the second term, the maximum error falls to -0.40% for the sphere, -0.20% for the cylinder and -0.05% for the infinite slab.

3.2. First approximations to the Biot number in other geometries

As can be seen in Appendix B, for a paralellepiped and a finite cylinder, equation (8) can be generalized to the equation:

$$Bi \approx \delta^2 \left[\frac{1}{(\Gamma + 1)} + \frac{2}{K_\delta \delta_M^2} \times \frac{\delta^2}{(\delta_M^2 - \delta^2)} \right] \tag{9}$$

where

$$K_\delta = \frac{\sum \omega_j^2 \delta_{Mj}^2}{\sum \omega_j^3 \delta_{M,j}^2} = \frac{\delta_M^2}{\sum \omega_j^3 \delta_{M,j}^2} \tag{10}$$

Here, δ is no longer a solution of boundary equations but responds to the following expression:

$$\delta^2 = \sum \omega_j^2 \delta_j^2 \tag{11}$$

And therefore:

$$\delta_M^2 = \sum \omega_j^2 \delta_{Mj}^2 \tag{12}$$

$\Gamma + 1$ can be written as:

$$\Gamma + 1 = \sum \omega_j (\Gamma_j + 1) \tag{13}$$

Where $\omega_j = R/X_j$ are the shape ratios and the components $\delta 0_j$ are the relevant boundary solutions. In equations (11) to (13) the summation is extended to match the number of component geometries.
Equation (9) generalizes equation (8) for parallelepiped and finite cylinder. In fact, for elementary geometries $K_\delta = 1$ and this equation matches equation (8), corresponding to elementary geometries. As seen in this equation, in addition to depending on the slope δ^2, Bi depends on three constants that depend only on geometric shape: $\Gamma + 1$, δ_M^2 and K_δ.
With this equation (9) the maximum error was found for a flattened square prism with a base ten times the height, in this case -7.49%; the mean deviation found for the parallelepiped and finite circular cylinder was -1.71%., and the average maximum deviation was -3.36% (this is the default deviation in all cases).

3.3. Ellipsoids

Given the general nature of equation (9), it seems reasonable to extend its use to other geometries in which the values of the three geometric constants occurring there can be determined. In the case of ellipsoids the constants that depend only on geometry can be calculated as follows:

3.3.1. Geometrical constant $\Gamma + 1$.

This constant can be calculated directly using exact equations both in triaxial ellipsoids [20] and in ellipsoids of rotation [21]. However, it can also be calculated simply and approximately using the approximate formula for the ellipsoid surface developed by Igathinathane and Chattopadhyay [22]-[23] which can be written as follows with the present nomenclature:

$$S = 4\pi(A_0 X_1^2 + A_1 X_1 X_3 + A_2 X_1 X_2 + A_3 X_3 X_2 + A_4 X_3 X_2^2 / X_1) \quad (14)$$

with:

$A_0 = -1.02274828 \times 10^{-2}$; $A_1 = 4.92988817 \times 10^{-1}$; $A_2 = 3.43560219 \times 10^{-1}$;
$A_3 = -5.29422959 \times 10^{-2}$ y $A_4 = 2.35999474 \times 10^{-1}$

Thus, the geometric constant $\Gamma + 1$ is defined as [20]:

$$\Gamma + 1 = \frac{SR}{V} \quad (15)$$

The volume of the ellipsoid is [20] and [21]:

$$V = \frac{4}{3}\pi \times X_1 \times X_2 \times X_3 \quad \text{poraqui} \quad (16)$$

Thus, substituting in (15) and rearranging terms gives:
A) Triaxial

$$\Gamma + 1 \approx 3\left(A_0 \frac{\omega_2}{\omega_1} + A_1\omega_2 + A_2 + A_3\omega_1 + A_4 \frac{\omega_1^2}{\omega_2} \right)$$

B) Prolate ($\omega_2 = 1;\ \omega_1 = R/L = \omega$)

$$\Gamma + 1 \approx 3\left(\frac{A_0}{\omega} + A_1 + A_2 + A_3\omega + A_4\omega^2 \right) \quad (17)$$

C) Oblate ($\omega_2 = \omega_1 = R/L = \omega$)

$$\Gamma + 1 \approx 3\left[A_0 + A_2 + (A_1 + A_3 + A_4)\omega \right] \quad (18)$$

3.3.2. Maximum slope δ_M^2

The value of δ_M^2 can be estimated by means of the equation of Smith et al. [24]:

$$\delta_M^2 = \pi^2 . \left(\frac{1}{4} + \frac{3}{8}\omega_2^2 + \frac{3}{8}\omega_3^2 \right) = \frac{\pi^2}{8}\left[2 + 3(\omega_2^2 + \omega_3^2) \right] \quad (19)$$

Where the shortest lenth is taken as the "x" coordinate.

3.3.3. Constant K_δ

For K_δ [25], as can be clearly seen in equation (10), the numerator and denominator are identical, except for the exponent to which ω_j are raised. Therefore, using this same criterion for the ellipsoid:

$$K_\delta = \frac{2+3\left(\omega_2^2+\omega_3^2\right)}{2+3\left(\omega_2^3+\omega_3^3\right)} \qquad (20)$$

4. Summary of the procedure

1) From the time-temperature data make the table Fo-Y (dimensionless).

2) Select the linear portion of the complete history ($Fo > 0.2$, [5]) and make the table Fo- $\ln Y$

3) Make linear regression to find the (minus) slope δ^2

4) Calculate the geometrical constant. The following particular values can be taken: $\Gamma + 1 = 1$ for flat plate, $\Gamma + 1 = 2$ for infinite cylinder and $\Gamma + 1 = 3$ for sphere. $\Gamma + 1 = \sum \omega_i(\Gamma_i + 1)$ for parallelepiped and finite cylinder. For other geometries Equation (15) can be applied:

$$\Gamma + 1 = \frac{S \times R}{V}$$

5) Calculate the maximum slope δ_M^2. The following particular values can be taken: $\delta_M^2 = (\pi/2)^2$= 2.4674 for flat plate, $\delta_M^2 = (2.4048)^2 = 5.7831$ for infinite cylinder and $\delta_M^2 = \pi^2$ =9-8696 for the sphere. For parallelepiped or finite cylinder apply the equation (12):

$$\delta_M^2 = \sum \omega_j^2 \delta_{Mj}^2$$

For other geometries, applay the Smith Equation (19):

$$\delta_M^2 = \pi^2\left(\frac{1}{4}+\frac{3}{8}\omega_2^2+\frac{3}{8}\omega_3^2\right)$$

6) Calculate the constant K_δ. In the case of elementary and cubic geometries (cube, cylinder of equal base that diameter or sphere) $K_\delta = 1$. For other geometries apply equation (10):

$$K_\delta = \frac{\sum \omega_j^2 \delta_{M,j}^2}{\sum \omega_j^3 \delta_{M,j}^2} = \frac{\delta_M^2}{\sum \omega_j^3 \delta_{M,j}^2}$$

7) Apply equation (9) to estimate Bi:

$$Bi \approx \delta^2\left[\frac{1}{(\Gamma+1)}+\frac{2}{K_\delta \delta_M^2}\times\frac{\delta^2}{(\delta_M^2-\delta^2)}\right]$$

8) Resolve the surface transfer coefficient h:

$$h = \frac{k \times Bi}{R}$$

5. Practical examples

5.1. Example I Elementary geometries

Awuah et al. [8] present values both for the slope and for the surface heat transfer coefficient derived from them, calculated in a 25.40 mm-diameter infinite cylinder made in Teflon with reference both to the thermal centre and to a point inside the cylinder located 3.39 mm below the surface. The thermophysical parameters that have to be considered are $k = 0.29\ \mathrm{W/m^oC}$ and $a = 1.35\times10^{-7}\ \mathrm{m^2/s}$.

As this is an infinite cylinder, $K_\delta = 1,\ \Gamma + 1 = 2$ and $\delta_M = 2.405$ so that substituting in equation (9) and resolving the surface transfer coefficient h:

$$h \approx \frac{k\cdot\delta^2}{R}\left[\frac{1}{2}+\frac{2}{5.783}\times\frac{\delta^2}{5.7832-\delta^2}\right]$$

Which gives the values of h calculated as functions of the value of the slope δ^2.

This can also be compared with the values derived by solving h in the following equation from Dincer [10], [11]:

$$Bi = \frac{hR}{k} = \frac{2.85\delta^2}{(6-\delta^2)}$$

Fig. 4 shows present (Eq. 9) and Dincer values, plotted as h_{cal}, compared with the values reported by Awuah et al., plotted as h_{exp} in the figure. The maximum deviation was -2.77% for the present paper and 5.51% for Dincer equation.

Fig. 4.

5.2. Example II. Regular geometries

This example is the reverse of the approach in the following example by Cleland and Earle [19] whose original proposition is: "It is required to cool blocks of cheddar cheese of dimensions 0.30 m x 0.38 m x 0.56 m. […]. The surface heat transfer coefficient taking account of resistance in the cheese carton wall, and in the air stream, is $13\ \mathrm{Wm^{-2}K^{-1}}$. Thermal properties of the cheese are $k = 0.42\ \mathrm{Wm^{-1}K^{-1}}$ and $C = 3.74 \times 10^6\ \mathrm{Jm^{-3}K^{-1}}$."

As the cheese may be taken to be a parallelepiped of dimensions $2X_1 = 0.56\ m$, $2X_2 = 0.38\ m$, $2X_3 = 0.30\ m$, it may be considered as a compound shape formed by the intersection of three infinite slabs. The reference length is thus $R = X_3 = 0.15\ m$ and therefore:

$$\omega_1 = \frac{R}{X_1} = \frac{0.15}{0.28} = 0.54$$

$$\omega_2 = \frac{R}{X_2} = \frac{0.15}{0.19} = 0.79$$

And the exact value $\delta^2 = 3.38$ will be found.

Present paper: Inverse solution using the present model (Eq. 9)

In the present case the proposition is as follows: In chilling of a block of cheddar cheese of dimensions 0.30 m x 0.38 m x 0.56 m, whose thermal properties are $k = 0.42\ \mathrm{Wm^{-1}K^{-1}}$ and $C = 3.74\times10^6\ \mathrm{Jm^{-3}K^{-1}}$, the slope of the straight part of the cooling curve obtained by regression from the time/temperature table is $\delta^2 = 3.38$. We are asked to estimate the surface heat transfer coefficient. For the infinite slab: $\Gamma_i + 1 = 1$ and $\delta^2_{M,i} = (\pi/2)^2 = 2.4674$, and as seen above, $\omega_1 = 0.54$ and $\omega_2 = 0.79$. Hence (equations 12, 13 and 10):

$$\delta_M^2 = \left(\frac{\pi}{2}\right)^2 (1 + \omega_2^2 + \omega_3^2) = 2.47(1 + 0.79^2 + 0.54^2) = 4.71$$

$$\Gamma + 1 = 1 + \omega_2 + \omega_3 = 1 + 0.79 + 0.54 = 2.33$$

$$K_\delta = \frac{\delta_M^2}{\sum \delta_{M,i}^2 \omega_i^3} = \frac{\sum \omega_i^2}{\sum \omega_i^3} = \frac{1 + 0.79^2 + 0.54^2}{1 + 0.79^3 + 0.54^3} = 1.16$$

Given that $\delta^2 = 3.38$, substituting in equation (9):

$$Bi \approx 3.38 \times \left[\frac{1}{2.33} + \frac{1}{1.16} \times \frac{2}{4.71} \times \frac{3.38}{4.71 - 3.38}\right] = 4.61$$

Therefore:

$$h = \frac{Bi \times k}{R} = \frac{4.61 \times 0.42}{0.15} = 12.90\ \mathrm{Wm^{-2}K^{-1}}$$

Since the real value is $h = 13\ \mathrm{Wm^{-2}K^{-1}}$, the error is -0.77%

5.3. Example III. Other geometries

The data are from experiments conducted on cherimoya to determine the effect of thermal shocks on the ripening process, and particularly on softening[*].

Thermal treatments were applied in a cabin with water spraying to permit strict control of temperature and relative humidity. The treatment was performed at an air temperature of 42ºC and 80% relative humidity until the thermal centre reached 40ºC, with real-time temperature recording for 60 minutes. Cherimoyas weighing 500 grams at an initial temperature of 15.6 ºC were placed on trays with thermocouples inserted in the peduncular region and located on the floral axis of the fruit (thermal centre) with 4 replicates per treatment.

The principal diameters of the cherimoya specimen used in this example were approximately: Equatorial diameter $2X_2 = 2X_3 = 9.44\,\text{cm}$, and maximum longitudinal diameter $L = 2X_1 = 10.17\ \text{cm}$. The measured volume was $V = 482.34\ \text{cm}^3$. The density was therefore:

$$\rho = \frac{M}{V} = \frac{500\times10^{-3}\ \text{Kg}}{482.34\times10^{-6}\ \text{m}^3} = 1036.62\ \text{Kg m}^{-3}$$

The composition taken for the cherimoya per 100 g was [26]: $x_{\text{Water}} = 73.5\,\text{g}$; $x_{\text{Prot}} = 1.3\,\text{g}$; $x_{\text{Carboh}} = 24.0\,\text{g}$; $x_{\text{Ash}} = 0.80\,\text{g}$, which calculating by difference gives a fat content of $x_{fat} = 100 - 99.6 = 0.4\,\text{g}$. These values can be used to calculate the value of the thermophysical parameters [27], [28] and thus obtain the following values: Thermal conductivity $k = 0.545\ \text{W m}^{-1}\ \text{K}^{-1}$; Thermal diffusivity $a = 1.503\times10^{-7}\ \text{m}^2\ \text{s}^{-1}$

From the original time (minutes) – temperature (ºC) table, together with these thermophysical parameters, it is possible to derive the $Fo - Y$ table (dimensionless), which is shown in Fig. 5 on a semi-logarithmic scale, where the linear portion is clearly visible (in this case $Fo > 0.2$). The slope in this zone (with the sign changed) derived by regression, was: $\delta^2 = 5.458$, with a coefficient $R^2 = 0.990$. It is required calculate the surface transfer coefficient of the experiment.

Fig. 5.

For the purposes of this example, the cherimoya may be considered as a prolate spheroid whose volume must be the volume of the real fruit. The radius is the lesser of the two semi-thicknesses so that the area of the smallest circular section of the equivalent ellipsoid is equal to the area of the corresponding smallest real section [24], [25]: hence $X_2 = X_3 = R = 4.72\ \text{cm} = 0.0472\ \text{m}$; $\omega_2 = R/X_2 = 1$. Since the volume of the ellipsoid of revolution is:

$$V = \frac{4}{3}\pi R^2 X_1$$

resolving X_1 gives:

$$X_1 = \frac{3}{4}\frac{V}{\pi\cdot R^2} = \frac{3}{4\pi}\times\frac{4.8234\times10^{-4}\ \text{m}^3}{0.0472^2\ \text{m}^2} = 0.0516\ \text{m}$$

The dimensional ratio is:

$$\omega_1 = \omega = \frac{R}{X_1} = \frac{0.0472}{0.0516} = 0.915$$

To calculate the geometric constant $\Gamma + 1$ the approximate equation (17) is used:

$$\Gamma + 1 \approx 3\times\left(\frac{A_0}{\omega} + A_1 + A_2 + A_3\omega + A_4\omega^2\right)$$

[*] Project of the Instituto del Frío (nowadays Institute of Food Science, Technology and Nutrition) financed by the National Plan CICYT. ALI96-1207-CO2-01

giving:

$$\Gamma + 1 = 2.923$$

and the geometric constants δ_M^2 (eq. 19) and K_δ (eq. 20):

$$\delta_M^2 \approx \frac{\pi^2}{8}\left[2 + 3 \times \left(1 + 0.915^2\right)\right] = 9.265$$

$$K_\delta \approx \frac{2 + 3\left(1 + 0.915^2\right)}{2 + 3\left(1 + 0.915^3\right)} = 1.029$$

Hence, the estimated Biot number is (eq. 9):

$$Bi = 5.458\left[\frac{1}{2.923} + \frac{1}{1.029} \times \frac{2}{9.265} \times \frac{5.458}{\left(9.265 - 5.458\right)}\right] = 3.508$$

And therefore the estimated surface transfer coefficient is:

$$h = \frac{Bi \times k}{R} = \frac{3.508 \times 0.545}{0.0472} = 40.504 \ \mathrm{Wm^{-2}K^{-1}}$$

How to check the validity of this result? Since in this case the surface heat transfer coefficient is not known, it must be checked by calculating the value of the slope δ^2 corresponding to this value of the newly-estimated Biot number and comparing it with the experimental value. In this connection [25] provide the following interpolation equation to calculate δ^2:

$$\frac{\delta_M^2}{\delta^2} = \left(1 + \frac{2}{K_\delta Bi}\right).\left(1 + \frac{K}{0{,}975.Bi^{1{,}25} + 1}\right) \qquad (21)$$

With:

$$K = \frac{K_\delta . \delta_M^2}{2.\left(\Gamma + 1\right)} - 1 \qquad (22)$$

As can be seen, equation (21) exactly reflects the asymptotic trends when $Bi \to 0$ and when $Bi \to \infty$. The maximum deviation found for δ^2 in the three elementary geometries was 1%, and for the square-based straight rectangular prism and the elongated circular cylinder it was always less than or in the region of 2%.

Thus, substituting the values in the example gives:

$\delta^2 = 5.405$

As noted in the data for this example, the value derived directly from the time-temperature table is $\delta_{exp}^2 = 5.458$, and hence the difference is -0.96%.

Lin et al. [29]-[31] propose a method for calculating chilling times of three-dimensional shapes. The method is essentially based on the first-term approximation to the analytical solution for the convective cooling of a sphere which, when adapted to our nomenclature, can be written:

$Y = A\ exp\left(-E\delta_{sph}^2 Fo/3\right)$

Where E is the equivalent heat transfer dimensionality [19] and δ_{sph} is the first root of the transcendental equation for a sphere. For $= 3.508$, $\delta_{sph} = 2.382$ and for this example we deduce $E = 3.201$ and hence the value of δ^2 estimated by this method for $Bi = 3.508$ is

$$\delta^2 = 3.201\frac{2.382^2}{3} = 6.054$$

The deviation with respect to the experimental value is 10.91%

Fig. 5 shows the temperature history in the cherimoya blanching experiment. In this figure is compared the slope δ^2 obtained by linear regression with the slope obtained by equation (21) and the slope δ^2 deduced using the equation of Lin et al. for the same Biot number. Since only the values of the slope are compared, in both cases the lag factor is taken to minimize the error for the corresponding slope.

6. Conclusions

1) If $\psi(\delta)$ is the spatial component of the solution in Fourier series, exact numeric series can be deduced for the functions $1/\psi(\delta)$ y $-\psi'(\delta)/\psi(\delta)$

2) A practical consequence of the above is that a new exact numerical series can be deduced for the Biot number for the three elementary geometries.

3) This series can be truncated to its first term to achieve a general and accurate first approximation for indirect estimation of the heat transfer coefficient in elementary geometries.

4) The maximum error introduced in the inverse calculation of the Biot number with this approximation is less than 1.8% in the three elementary geometries.

5) This first approximation can be generalized to indirectly estimate the the heat transfer coefficient in regular geometries (parallelepíped and finite cylinder) to give a very general expression in which elementary geometries fit as a particular case.

6) The maximum error was found for a flattened square prism with a base ten times the height, in this case -7.5%; the mean deviation found for the parallelepiped and finite circular cylinder was -1.71%, and the average maximum deviation was -3.36%.

7) Because the approximation described in conclusion 5 is so general, it is suggested that the equation may be applied to ellipsoids.

Acknowledgements.

The data for Example III were taken from the project entitled "Strategies to optimize the marketing of cherimoya using low-cost, non-pollutant post-harvest technologies" directed by Dr. Rafael Alique of the Department of Plant Foods Science and Technology, Instituto del Frío (CSIC), Jose Antonio Novais, 10, 28040 Madrid, Spain., in coordination with the Department of Biochemistry and Molecular Biology of the Faculty of Pharmacy, University of Granada. CICYT. ALI96-1207-CO2-01

Appendix A. Deduction of the numerical series

The deduction of series (5), (6) and (7) in paragraph 2 of this paper involves two other series, which need to be substantiated beforehand. To address that issue, this Appendix is divided into three separate parts. The first sets out the deduction of these two prior series, and the second and third series (5), (6) and (7), which are the actual subject of this paper.

Part one: Prior series (derived from the no heat generation case)

In the no internal heat generation case the separate-variables solution to the Fourier equation in homogeneous and isotropic elementary-geometry solids with uniform initial temperature and with boundary conditions of the third type can be written dimensionlessly as follows [12]:

$$Y = \sum_{n=1}^{\infty} A_{n,0}\psi(\delta_n x)e^{-\delta_n^2 Fo} \qquad \text{(A-1)}$$

$A_{n,0}$ are the expansion coefficients

$$A_{n,0} = \frac{2Bi}{\psi_{\delta_n}\left[\delta_n^2 + Bi^2 - (\Gamma - 1)Bi\right]} \qquad \text{(A-2)}$$

and

$$\psi_{\delta_n} = \psi(\delta_n)$$

δ_n are the solutions to the transcendental boundary condition equation:

$$-\delta\psi'_{\delta} = Bi\,\psi_{\delta} \qquad \text{(A-3)}$$

There are two important special cases of equation (A-1). One is the thermal centre of the solid, where $x = 0$, and therefore $\psi(0) = 1$:

$$Y_c = \sum_{n=1}^{\infty} A_{n,0} e^{-\delta_n^2 Fo} \tag{A-4}$$

The second is the mass average value:

$$\overline{Y} = \sum_{n=1}^{\infty} A_{n,0} \overline{\psi}_{\delta_n} \cdot e^{-\delta_n^2 Fo} \tag{A-5}$$

Where

$$\overline{\psi}_{\delta} = \int_{x=0}^{x=1} \psi(\delta \cdot x) dx = \frac{-(\Gamma+1)}{\delta} \cdot \psi'_{\delta} \tag{A-6}$$

And

$$A_{n,0} \overline{\psi}_{\delta_n} = \overline{A}_{n,0} = \frac{2Bi^2(\Gamma+1)}{\delta_n^2 \left[\delta_n^2 + Bi^2 - (\Gamma-1)Bi\right]} \tag{A-7}$$

At $t = 0$, $Fo = 0$ and hence $e^{-\delta_n^2 \cdot Fo} = 1$ and, by construction, both for the centre and for the mass average value the temperature is uniform, ie the dimensionless ratio of temperature difference is equal to 1. Therefore Y_c and $\overline{Y}$ can be writen:

$$Y_c = \sum_{n=1}^{\infty} A_{n,0} = 1 \tag{A-8}$$

$$\overline{Y} = \sum_{n=1}^{\infty} \overline{A}_{n,0} = 1 \tag{A-9}$$

For the case $Bi \to \infty$, (A-2) and (A-7) take the following values:

$$\left(A_{n,0}\right)_{Bi=\infty} \equiv A_{n,0,M} = \frac{-2}{\delta_{n,M} \psi'_{n,M}} \tag{A-10}$$

$$\left(\overline{A}_{n,0}\right)_{Bi\to\infty} = \overline{A}_{n,0,M} = \frac{2(\Gamma+1)}{\delta_{n,M}^2} \tag{A-11}$$

$\delta_{n,M} = \delta_n$ for $Bi = \infty$ and $\psi'_{n,M} = \psi'(\delta_{n,M})$.

Hence, substituting in (A-8) and (A-9) this gives the two numerical series:

$$\sum \frac{-1}{\delta_{n,M} \psi'_{n,M}} = \frac{1}{2} \tag{A-12}$$

$$\sum \frac{1}{\delta_M^2} = \frac{1}{2(\Gamma+1)} \tag{A-13}$$

This series (A-13) increases for all cases to the value of convergence $1/[2(\Gamma+1)]$, and is valid for all three geometries. In contrast, the series (A-12) (which is an alternating series) is valid only for the flat plate and the infinite cylinder.

The terms of the particular expressions of series (A-12) and (A-13) for the flat plate and the sphere can be rearranged to lead to well-known numerical series included in handbooks of mathematical tables [32]. However, the series (A-12) and (A-13) are also valid in the case of the infinite cylinder. In this case $\psi(x) = J_0(x)$ and $\psi'(x) = -J_1(x)$, and therefore the series takes the form:

$$\sum \frac{1}{\delta_{n,M,Cyl} J_{1,n,M}} = \frac{1}{2}$$

$$\sum \frac{1}{\delta_{n,M,Cyl}^2} = \frac{1}{2(\Gamma+1)} = \frac{1}{4}$$

which can be verified without difficulty, although the convergence is very slow

Part two: Series derived from the linear heat generation case

In the case of an internal heat source linearly dependent on temperature, the separate-variables solution to the Fourier equation in homogeneous and isotropic elementary-geometry bodies with boundary conditions of the third type leads to infinite series which, expressed in dimensionless terms, can generally be written as follows [33]:

$$Y - Y_s = \sum_{n=1}^{\infty} A_n \psi(\delta_n x) \cdot e^{-(\delta_n^2 - \alpha^2) Fo} \qquad \text{(A-14)}$$

where Y_s is the steady state solution :

$$Y_s = \frac{T_s - T_{ex}}{\Delta T_0} = \frac{\beta}{\alpha^2}\left[\frac{Bi.\psi(\alpha x)}{\alpha \psi'_\alpha + Bi\,\psi_\alpha} - 1\right] \qquad \text{(A-15)}$$

and

$$\psi_\alpha = \psi(\alpha) \text{ and } \psi'_\alpha = \psi'(\alpha) \qquad \text{(A-16)}$$

The expansion coefficients A_n are:

$$A_n = A_{n,0}\left(1 - \frac{\beta}{\delta_n^2 - \alpha^2}\right) \qquad \text{(A-17)}$$

$A_{n,0}$ are the expansion coefficients for the no internal heat generation case (equation A-2)

$$A_{n,0} = \frac{2Bi}{\psi_{\delta_n}\left[\delta_n^2 + Bi^2 - (\Gamma - 1)Bi\right]}$$

α^2 and β are the two parameters that define the internal heat source, dimensionlessly expressed:

$$\alpha^2 = \frac{A_1 R^2}{k} \qquad \text{(A-18)}$$

$$\beta = \frac{B_0 \cdot R^2}{k \cdot \Delta T_0} \qquad \text{(A-19)}$$

In these equations A_0 $(\mathrm{J\,m^{-3}s^{-1}})$ and A_1 $(\mathrm{J\,m^{-3}s^{-1}K^{-1}})$ are the constants of the linear heat source (not to be confused with the coefficients of expansion of the series, equations (A-2) and equation (A-17) and $B_0 = A_0 + A_1 T_{ex}$. δ_n are the solution to the classical transcendental equation (as in the no heat generation case).

As in the first part of this appendix, the main interest falls on the thermal centre and on the mass average solutions:

For the thermal centre ($x = 0$; $\psi(0) = 1$):

$$Y_c(Fo) = Y_{c,s} + \sum_{n=1}^{\infty} A_n e^{-(\delta_n^2 - \alpha^2) Fo} \qquad \text{(A-20)}$$

With the steady state solution:

$$Y_{c,s} = \frac{\beta}{\alpha^2}\left[\frac{Bi}{\alpha \psi'_\alpha + Bi\,\psi_\alpha} - 1\right] \qquad \text{(A-21)}$$

For the mass average:

$$\overline{Y}(Fo) = \overline{Y}_s + \sum_{n=1}^{\infty} \overline{A}_n e^{-(\delta_n^2 - \alpha^2) \cdot Fo} \qquad \text{(A-22)}$$

where $\overline{Y}_s$ is the steady state value corresponding to the mass average temperature.

$$\bar{Y}_s = -\frac{\beta}{\alpha^2}\left[\frac{(\Gamma+1)}{\alpha}\frac{Bi\,\psi'_\alpha}{\alpha\psi'_\alpha + Bi\,\psi_\alpha}+1\right] \qquad \text{(A-23)}$$

and the expansion constants $\bar{A}_n$:

$$\bar{A}_n = \bar{A}_{n,0}\cdot\left(1-\frac{\beta}{\delta_n^2-\alpha^2}\right) \qquad \text{(A-24)}$$

where $\bar{A}_{n,0} = A_{n,0}\bar{\psi}_{\delta_n}$ is the value quoted in equation (A-7)

$$\bar{A}_{n,0} = \frac{2Bi^2(\Gamma+1)}{\delta_n^2\left[\delta_n^2+Bi^2-(\Gamma-1)Bi\right]}$$

As in the no heat generation case, the initial temperature is constant, and hence $Y=1$ both for the centre and for the mass average value. The following equations are then valid from (A-20) and (A-22):

$$Y_c(0) = Y_{c,s} + \sum_{n=1}^{\infty} A_n = 1 \qquad \text{(A-25)}$$

$$\bar{Y}(0) = \bar{Y}_s + \sum_{n=1}^{\infty} \bar{A}_n = 1 \qquad \text{(A-26)}$$

Numerical series derived from the centre equation (A-25)

By substituting equations (A-21) and (A-17) in (A-25):

$$Y_c = \frac{\beta}{\alpha^2}\left[\frac{Bi}{\alpha\psi'_\alpha + Bi\,\psi_\alpha}-1\right] + \sum_{n=1}^{\infty} A_{n,0}\left(1-\frac{\beta}{\delta_n^2-\alpha^2}\right) = 1 \qquad \text{(A-27)}$$

Given that

$$\sum_{n=1}^{\infty} A_{n,0}\left(1-\frac{\beta}{\delta_n^2-\alpha^2}\right) = \sum_{n=1}^{\infty} A_{n,0} - \sum_{n=1}^{\infty}\frac{A_{n,0}\beta}{\delta_n^2-\alpha^2}$$

given that (equation (A-8))

$$\sum_{n=1}^{\infty} A_{n,0} = 1$$

And simplifying both sides of the equation, (A-27) can be rewritten:

$$\frac{Bi}{\alpha\psi'_\alpha + Bi\,\psi_\alpha} - 1 = \sum_{n=1}^{\infty} A_{n,0}\frac{\alpha^2}{\delta_n^2-\alpha^2}$$

And for $Bi=\infty$

$$\frac{1}{\psi_\alpha} - 1 = \sum_{n=1}^{\infty} A_{n,0,M}\frac{\alpha^2}{\delta_{n,M}^2-\alpha^2}$$

Finally, inserting equation (A-10):

$$A_{n,0,M} = \frac{-2}{\delta_{n,M}\psi'_{n,M}}$$

and resolving the function ψ_α :

$$\frac{1}{\psi_\alpha} = 1 + \sum\frac{-2}{\delta_{n,M}\psi'_{n,M}}\frac{\alpha^2}{\delta_{n,M}^2-\alpha^2} \qquad \text{(A-28)}$$

Tis equation is valid for the three elementary geometries. The convergence of this series is much more rapid than the series (A-12) and (A-13).

In the flat plate and infinite cylinder cases, the series (A-12) is valid and therefore the numeric value 1 can be replaced by the series $1=\sum A_{n,M,0}$. Rearranging terms, the series (A-28) can be written more simply in the flat plate and infinite cylinder cases, thus:

$$\frac{1}{\psi_a}=\sum_{n=1}^{\infty}\frac{-2}{\delta_{n,M}\psi'_{n,M}}\left(\frac{\delta_{n,M}^2}{\delta_{n,M}^2-\alpha^2}\right) \qquad \text{(A-29)}$$

However, when the value 1 is replaced by the series $1=\sum A_{n,0}$ the convergence is necessarily slowed down, as in practice, in the partial sums of the series a concrete value (the value 1) is replaced by a number of terms from its series.

Series derived from the mass average equation (A-26)

Operating as in the case of the centre, replacing (A-23):

$$\overline{Y}_s=-\frac{\beta}{\alpha^2}\left[\frac{(\Gamma+1)}{\alpha}\frac{Bi\,\psi'_\alpha}{\alpha\psi'_\alpha+Bi\,\psi_\alpha}+1\right]$$

and (A-24)

$$\overline{A}_n=\overline{A}_{n,0}\cdot\left(1-\frac{\beta}{\delta_n^2-\alpha^2}\right)$$

in the mass average equation (A-26):

$$\overline{Y}(0)=\overline{Y}_s+\sum_{n=1}^{\infty}\overline{A}_n=1$$

$$-\frac{\beta}{\alpha^2}\left[\frac{Bi(\Gamma+1)}{\alpha\psi'_\alpha+Bi\,\psi_\alpha}\frac{\psi'_\alpha}{\alpha}+1\right]+\sum_{n=1}^{\infty}\overline{A}_{n,0}\left(1-\frac{\beta}{\delta_n^2-\alpha^2}\right)=1$$

And in the case $Bi=\infty$, considering (A-9):

$$\sum\overline{A}_{n,0}=1$$

and operating as in the previous case, the result is:

$$\frac{-\psi'_\alpha}{\psi_\alpha}=\frac{\alpha}{(\Gamma+1)}\left[1+\sum_{n=1}^{\infty}\overline{A}_{n,M,0}\frac{\alpha^2}{\delta_{n,M}^2-\alpha^2}\right]$$

and since (equation (A-11):

$$\overline{A}_{n,0,M}=\frac{2(\Gamma+1)}{\delta_{n,M}^2}$$

Finally yields the following series for the ratio ψ'_α/ψ_α :

$$\frac{-\psi'_\alpha}{\psi_\alpha}=\frac{\alpha}{(\Gamma+1)}\left[1+\sum_{n=1}^{\infty}\frac{2(\Gamma+1)}{\delta_{n,M}^2}\frac{\alpha^2}{\delta_{n,M}^2-\alpha^2}\right] \qquad \text{(A-30)}$$

The convergence of this series is very rapid, and in practice 4 or 5 terms are sufficient to determine the value very precisely.

Here again, the constant value 1 can be replaced by the series $1=\sum\overline{A}_{n,M,0}$, which in this case is valid for all three geometries, as seen in equation (A-11), in Part One of this Appendix. The result is a general one, which is thus simpler but obviously slower in terms of convergence. It is as follows:

$$\frac{-\psi'_\alpha}{\psi_\alpha}=2\sum_{n=1}^{\infty}\frac{\alpha}{\delta_{n,M}^2-\alpha^2} \qquad \text{(A-31)}$$

As in the case of series (A-12) and (A-13), the particular expressions of series (A-29) and (A-31) for a flat plate and a sphere, and of series (A-30) for a sphere, terms can be rearranged to lead to known series [32].

However, it is easy to see that the four series (A-28) to (A-31) can be applied in all cases, including the infinite cylinder.

Part Three. Consequence of series (A-30) y (A-31). Biot number.

The series (A-30) and (A-31) have a practical application in the inverse calculation of the Biot number for a given slope δ^2 in the case of the three basic geometries. In fact, from purely mathematical considerations, α can be considered simply as the real independent variable (x) depending on which the functions $\psi(x)$ and $\psi(x)/\psi'(x)$ can be calculated according to the series (A-28) to (A-31). This specific variable can take the particular value $x=\delta$, so that these series can be used to calculate these functions for the value δ. This gives:

$$\frac{1}{\psi(\delta)} = 1 + \sum \frac{-2}{\delta_{n,M}\psi'_{n,M}} \frac{\delta^2}{\delta_{n,M}^2 - \delta^2} \qquad \text{(A-32)}$$

$$\frac{1}{\psi(\delta)} = \sum_{n=1}^{\infty} \frac{-2}{\delta_{n,M}\psi'_{n,M}} \left(\frac{\delta_{n,M}^2}{\delta_{n,M}^2 - \delta^2} \right) \qquad \text{(A-33)}$$

$$\frac{-\psi'(\delta)}{\psi(\delta)} = \frac{\delta}{(\Gamma+1)} \left[1 + \sum_{n=1}^{\infty} \frac{2(\Gamma+1)}{\delta_{n,M}^2} \frac{\delta^2}{\delta_{n,M}^2 - \delta^2} \right] \qquad \text{(A-34)}$$

$$\frac{-\psi'(\delta)}{\psi(\delta)} = 2\sum_{n=1}^{\infty} \frac{\delta}{\delta_{n,M}^2 - \delta^2} \qquad \text{(A-35)}$$

If, in heat conduction with boundary conditions of the third type, the value δ is the solution to the transcendental equation (A-3), solving $-\psi'_\delta/\psi_\delta$

$$-\frac{\psi'_\delta}{\psi_\delta} = \frac{Bi}{\delta}$$

And substituting in (A-34) and (A-35), it is concluded that, for the three basic geometries, the Biot number can be written as the expansion of the following two numeric series:

$$Bi = \frac{\delta^2}{(\Gamma+1)} \left[1 + \sum_{n=1}^{\infty} \frac{2(\Gamma+1)}{\delta_{n,M}^2} \frac{\delta^2}{\delta_{n,M}^2 - \delta^2} \right] \qquad \text{(A-36)}$$

$$Bi = 2\sum_{n=1}^{\infty} \frac{\delta^2}{\delta_{n,M}^2 - \delta^2} \qquad \text{(A-37)}$$

Although both series are valid, for practical purposes of calculating with the first approximation, only the series (A-36) will be considered since it converges very quickly, while series (A-37) converges much more slowly.

Appendix B. Approximation to the Biot number in parallelepiped and finite cylinder

Series (9) is mathematically exact for elementary geometries, and hence also its first approximation (10) is valid for these geometries. The idea is , then, to arrive at a generalization of this approximation (10) for other convex geometries.

Analysis of equation (10):

$$Bi = \frac{hR}{k} \approx \delta^2 \left[\frac{1}{(\Gamma+1)} + \frac{2}{\delta_M^2} \times \frac{\delta^2}{\delta_M^2 - \delta^2} \right]$$

In this equation, if $Bi \to 0$, $\delta^2/(\delta_M^2 - \delta^2) \to 0$, and if $Bi \to \infty$ $\delta^2/(\delta_M^2 - \delta^2) \to \infty$. So, the asymptotes for $Bi \to 0$ and $Bi \to \infty$ are:

When $Bi \to 0$:

$$\frac{Bi}{\delta^2} \approx \frac{1}{(\Gamma+1)} \quad \text{(B-1)}$$

And for $Bi \longrightarrow \infty$:

$$\frac{Bi}{\delta^2} \approx \frac{2}{\delta_M^2} \frac{\delta^2}{\delta_M^2 - \delta^2} \quad \text{(B-2)}$$

That is, in the case of elementary geometries Bi/δ^2 can be written as the sum of its two asymptotes (eqs. B-1 and B-2). For very large values of Bi, such as $\delta^2 \approx \delta_M^2$, (B-2) this gives:

$$Bi \approx \frac{2\delta^2}{\delta_M^2 - \delta^2} \quad \text{(B-3)}$$

From which, by solving δ^2:

$$\delta^2 \approx \frac{\delta_M^2}{\left(1+\frac{2}{Bi}\right)} \quad \text{(B-4)}$$

Generalization to paralellepiped and finite cylinder

At the limit $Bi \to 0$, equation (B-1) generalizes to an equation that is formally identical for these regular geometries [25]:

$$Bi \approx \frac{\delta^2}{(\Gamma+1)} \quad \text{(B-5)}$$

Where in this case δ^2 has the following expression:

$$\delta^2 = \sum \omega_j^2 \delta_j^2 \quad \text{(B-6)}$$

And where for parallelepiped and finite cylinder $\Gamma + 1$ can be written as:

$$\Gamma + 1 = \sum \omega_j \left(\Gamma_j + 1\right) \quad \text{(B-7)}$$

Where $\omega_j = R/X_j$ are the shape ratios and the components δ_j are the relevant boundary solutions. In equations (B-6) and (B-7) the summation is extended to match the number of component geometries.

For a parallelepiped and a finite cylinder, at the limit $Bi \longrightarrow \infty$ equation (B-4) can be generalized in a first approximation in the form [25]:

$$\frac{1}{\delta^2} \approx \frac{1}{\delta_M^2}\left(1 + \frac{2}{K_\delta Bi}\right) \quad \text{(B-8)}$$

where

$$K_\delta = \frac{\sum \omega_j^2 \delta_{Mj}^2}{\sum \omega_j^3 \delta_{M,j}^2} = \frac{\delta_M^2}{\sum \omega_j^3 \delta_{M,j}^2} \quad \text{(B-9)}$$

In (B-8) the Biot number can be resolved, giving:

$$Bi \approx \frac{2}{K_\delta} \frac{\delta^2}{\delta_M^2 - \delta^2}$$

Which is a generalization of (B-3). The generalization of (B-2) will then be:

$$Bi \approx \frac{\delta^2}{\delta_M^2} \frac{2}{K_\delta} \frac{\delta^2}{\delta_M^2 - \delta^2} \quad \text{(B-10)}$$

As seen in the previous paragraph, in the case of elementary geometries the approximation is the sum of its two asymptotes $Bi \to 0$ and $Bi \to \infty$. Therefore, following the same criteria with the two asymptotic extremes (B-5) and (B-10):

$$Bi \approx \delta^2 \left[\frac{1}{(\Gamma+1)} + \frac{2}{K_\delta \delta_M^2} \times \frac{\delta^2}{(\delta_M^2 - \delta^2)}\right] \quad \text{(B-11)}$$

This equation generalizes equation (10) for a parallelepiped and a finite cylinder. Thus, for elementary geometries $K_\delta = 1$ and this equation matches the corresponding equation (10) for elementary geometries.

References

[1] H. Gröber, S. Erk, & U. Grigull, Transmisión del Calor, First Ed., Selecciones Científicas, Madrid, 1967, pp.15-17, 1967.

[2] H. Schlichting,. Teoría de la capa límite, Urmo, Bilbao, 1972, pp. 283-285 and 684-691.

[3] P.M. Beckett, A note on surface heat transfer coefficients, International Journal of Heat Mass Transfer 34 (8) (1991) 2165-2166.

[4] H.G. Kwon, S.D. Hwang, H.H. Cho, Measurement of local heat/mass transfer coefficients on a dimple using naphthalene sublimation, International Journal of Heat and Mass Transfer. 54 (2011) 1071–1080.

[5] F. Erdoğdu , A review on simultaneous determination of thermal diffusivity and heat transfer coefficient, Journal of Food Engineering 86 (2008) 453–459.

[6] A. Kondjoyan, A review on surface heat and mass transfer coefficients during air chilling and storage of food products, International Journal of Refrigeration 29 (2006) 863-875.

[7] B.A. Anderson, R.P. Singh, Effective heat transfer coefficient measurement during air impingement thawing using an inverse method. International Journal of Refrigeration 29 (2006) 281–293.

[8] G.B. Awuah, H.S. Ramaswamy, B.K. Simpson, Comparison of two methods for evaluating fluid-to-surface heat transfer coefficients, Food Research International, 28(3) (1995) 261-271.

[9] B.R. Becker, B.A. Fricke, Heat transfer coefficients for forced-air cooling and freezing of selected foods, International Journal of Refrigeration 27 (2004) 540–551.

[10] I. Dincer, Heat-transfer coefficients in hydrocooling of spherical and cylindrical food products, Energy 18(4) (1993) 335-340.

[11] I. Dincer, Determination of thermal diffusivities of cylindrical bodies being cooled, International Communications in Heat and Mass Transfer, 23 (5) (1996) 713-720.

[12] H.S. Carslaw, J.C. Jaeger, Conduction of Heat in Solids, second ed., Clarendon Press, Oxford, 1959, pp. 33-38.

[13] S. Chantasiriwan, Inverse heat conduction problem of determining time-dependent heat transfer coefficient, International Journal of Heat and Mass Transfer, 42(23) (1999) 4275-4285.

[14] F. Chunli,S. Fengrui, Y. Li, A Numerical Method on Inverse Determination of Heat Transfer Coefficient Based on Thermographic Temperature Measurement, Chinese Journal of Chemical Engineering, 16 (6) (2008) 901-908.

[15] W.P. Silva , C.M.D.P.S. Silva, V.S. Farias, D.D.P.S Silva, Calculation of the convective heat transfer coefficient and cooling kinetics of an individual fig fruit. Heat Mass Transfer 46 (3) (2010) 371–380

[16] W.P. Silva , C.M.D.P.S. Silva, P.L. Nascimento, J.E.F. Carmo, D.D.P.S. Silva, Influence of the geometry on the numerical simulation of the cooling kinetics of cucumbers. Spanish Journal of Agricultural Research 9 (1) (2011) 242-251

[17] X.T. Xiong, X.H. Liu, Y.M. Yan, H.B. Guo, A numerical method for identifying heat transfer coefficient, Applied Mathematical Modelling. 34 (7) (2010) 1930-1938.

[18] J. Rey Pastor, A. De Castro-Brzezicki, Funciones de Bessel, Dossat, Madrid, 1958, p.231.

[19] A.C. Cleland, R.L. Earle, A simple method for prediction of heating and cooling rates in solids of various shapes, International Journal of Refrigeration, 5 (1982) 98-106.

[20] K.A. Fikiin, A.G.Fikiin, Modèle numerique du refroidissement de matières alimentaires et dáutres corps solides de forme géométrique varièe, International Journal of Refrigeration, 12 (4) (1989) 224-231.

[21] W.M.Rohsenow, J.P. Hartnett, E.N. Gani, Handbook of Heat Transfer Fundamentals, second ed., McGraw Hill, New York ,1985, pp. 4.38, 4.39.

[22] C. Igathinathane, P.K. Chattopadhyay, Surface area of general ellipsoid shaped food materials by simplified regression equation method, Journal of Food Engineering. 46 (4) (2000) 257-266.

[23] C. Igathinathane, P.K. Chattopadhyay, Corrigendum to "Surface area of general ellipsoid shaped food materials by simplified regression equation method", Journal of Food Engineering, 85 (4) (2008) 639.

[24] R.E. Smith, G.L. Nelson, R.L. Henrickson, Analyses on Transient Heat Transfer from Anomalous Shapes, Trans. ASAE 10 (2) (1967) 236-244.

[25] F.J.Cuesta, M. Lamúa , Asymptotic modelling of the transient regime in heat conduction in solids with general geometry, Journal of Food Engineering. 24 (3) (1995) 295-320.

[26] T. Palma, J.M. Aguilera, D.W. Stanley, A review of postharvest events in cherimoya. Postharvest Biology and Technology, 2 (3) (1993) 187-208.

[27] Y. Choi, M.R. Okos, Effects of temperature and composition on the thermal properties of foods, in: L. Maguer & P. Jelen (Eds.), Food Engineering and Process Applications: Transport Phenomenon Vol. 1, Elsevier, New York, 1986, pp. 93–116.

[28] Thermal properties of foods, 1998, ASHRAE Refrigeration Handbook, ASHRAE, p. 8.2.

[29] Z. Lin, A.C. Cleland, D.J. Cleland, G.F. Serrallach, A simple method for prediction of chilling times: extension to three-dimensional irregular shapes, International Journal of Refrigeration, 19 (2) (1996) 107-114.

[30] Z. Lin, A.C. Cleland, D.J. Cleland, G.F. Serrallach, A simple method for prediction of chilling times: extension to three-dimensional irregular shapes, International Journal of Refrigeration, 19 (2) (1996) 95-106

[31] Z. Lin, A.C. Cleland, D.J. Cleland, G.F. Serrallach, Erratum to "A simple method for prediction of chilling times: extension to three-dimensional irregular shapes" [Int J Refrig 1996;19 (2):107-114]. International Journal of Refrigeration 23 (2000) 168.

[32] I.S. Gradshteyn, I.M. Ryzhik, Table of integrals, series, and products, Academic Press, 1980, pp. 7 and 36.

[33] F. J. Cuesta, M. Lamúa, Fourier series solution to the heat conduction equation with an internal heat source linearly dependent on temperature: Application to chilling of fruit and vegetables, Journal of Food Engineering. 90 (2) (2009) 291–299.

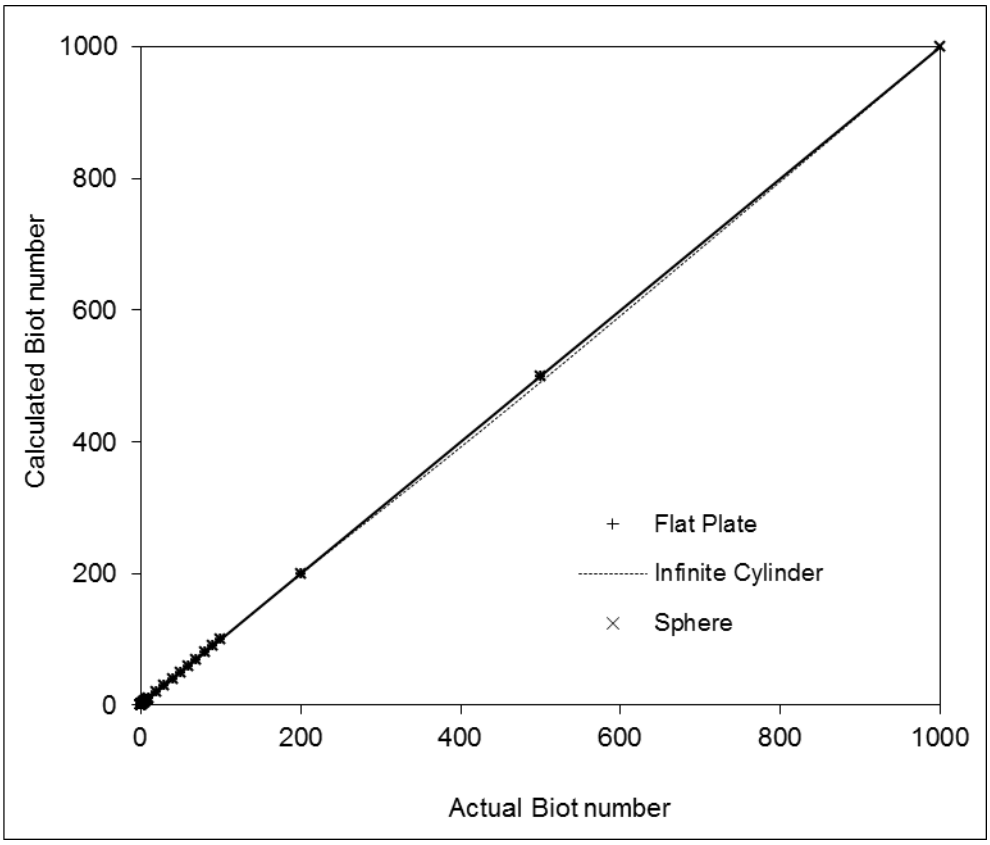

Fig. 1. Biot number calculated from series (7) versus the exact Biot number. The unbroken diagonal line reflects the Biot number versus itself.

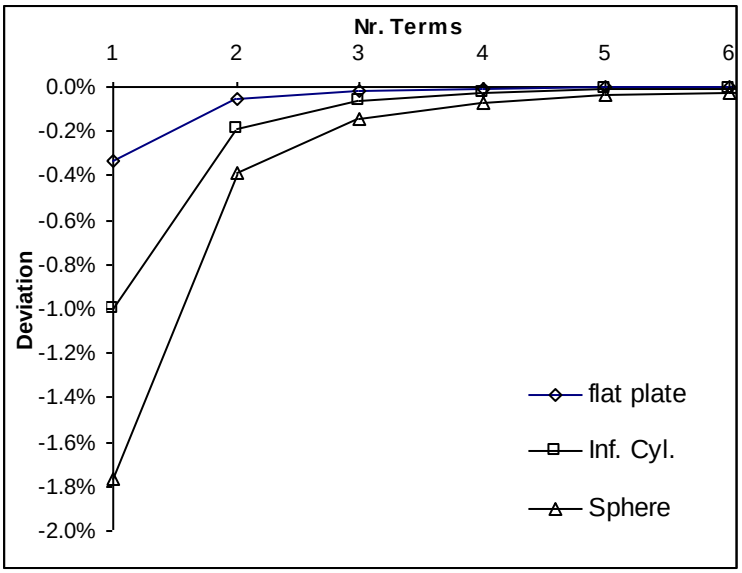

Fig. 2. Truncation error (%) of the partial series as a function of the number of terms taken for the sum. The reference Biot number is $Bi = 4$ in all three geometries.

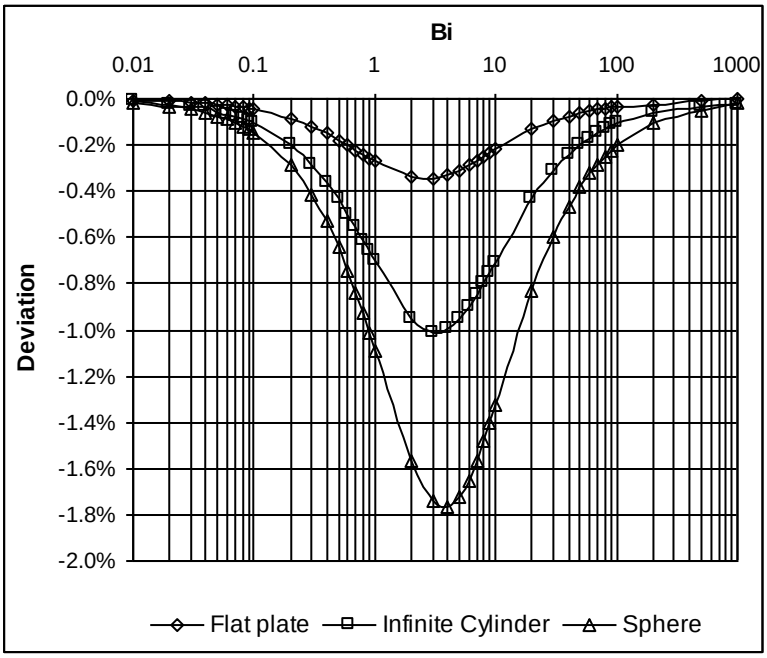

Fig. 3. Distribution of the error occurring when the complete series (Eq. 7) is substituted by its first partial series for elementary geometries (Eq. 8).

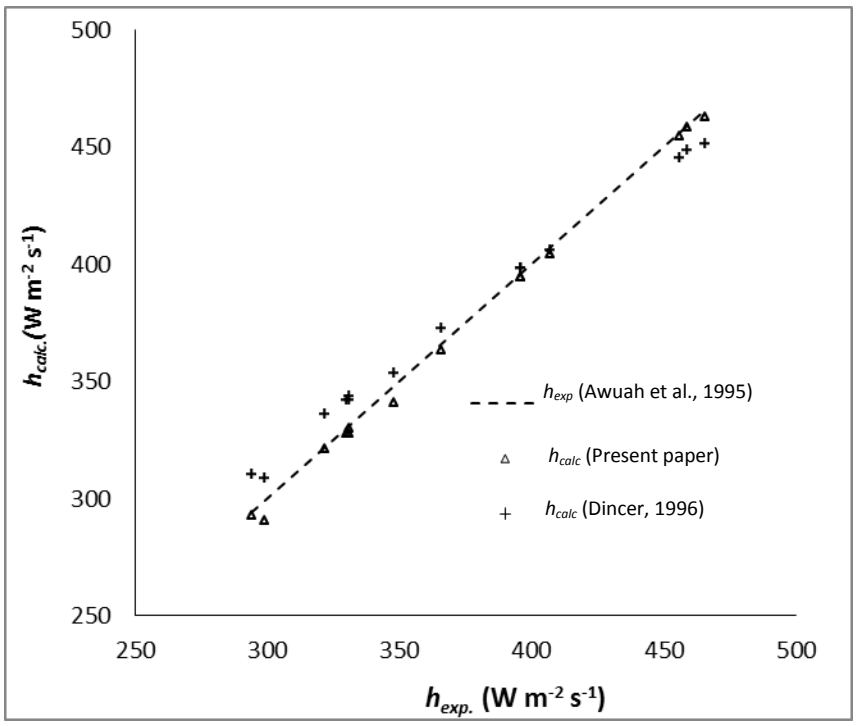

Fig. 4. Comparison of the estimated surface transfer coefficient (h_{calc}) versus experimental. ($h_{\exp}$): Dotted line = Values of Awuah et al. (1995); Triangles = Present paper; Crosses = Values calculated from Dincer (1996)

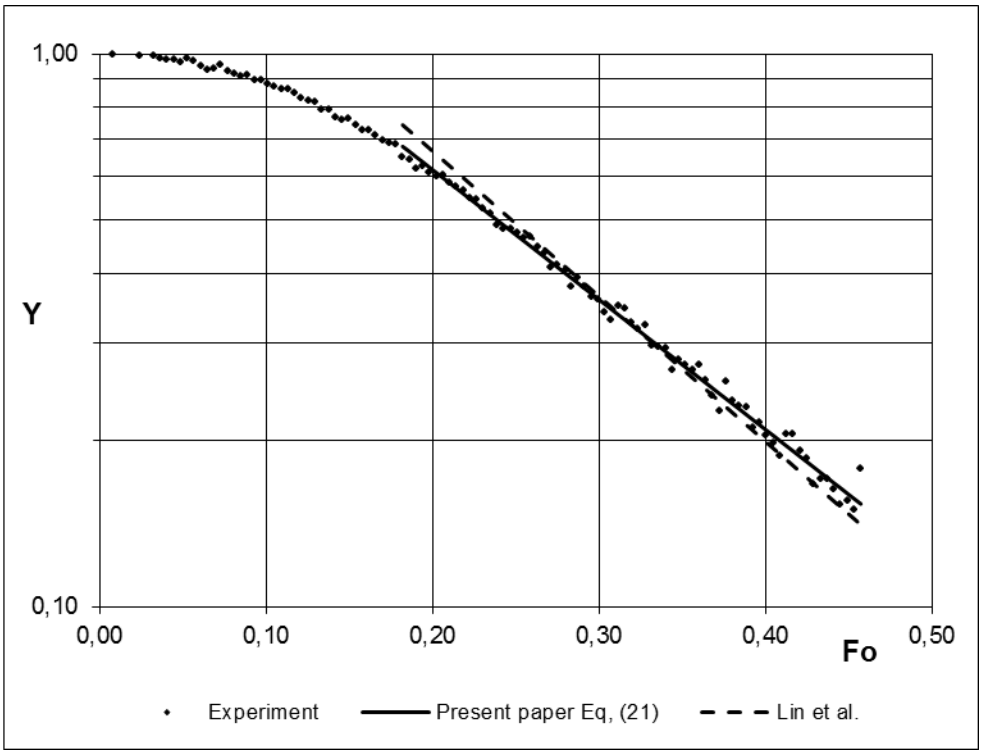

Fig. 5. Comparison of the slope δ^2 of the temperature history in cherimoya blanching experiment. The solid line represents the present paper approach (Eq. 21). The dotted line represents the Lin et al. (1996 a, b and 2000) approach. Only the values of the slope δ^2 are compared, and therefore the lag factor is taken in both cases to minimize the error in each one.

Table 1. First 20 roots $\delta_{n,M}$ and values of $J_1(\delta_{n,M})$ in an infinite cylinder

n	$\delta_{n,M}$	$J_1(\delta_{n,M})$
1	2,4048	0,5191
2	5,5201	-0,3403
3	8,6537	0,2715
4	11,7915	-0,2325
5	14,9309	0,2065
6	18,0711	-0,1877
7	21,2116	0,1733
8	24,3525	-0,1617
9	27,4935	0,1522
10	30,6346	-0,1442
11	33,7758	0,1373
12	36,9171	-0,1313
13	40,0584	0,1261
14	43,1998	-0,1214
15	46,3412	0,1172
16	49,4826	-0,1134
17	52,6241	0,1100
18	55,7655	-0,1068
19	58,9070	0,1040
20	62,0485	-0,1013